

# Highly Sensitive SERS Detection of As<sup>3+</sup> Ions in Aqueous Media using Glutathione Functionalized Silver Nanoparticles

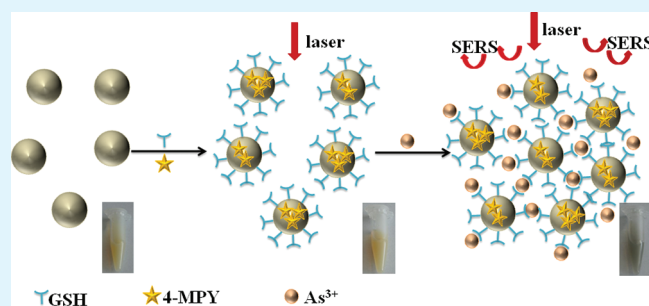
Jinglian Li,<sup>†,‡</sup> Lingxin Chen,<sup>\*,†</sup> Tingting Lou,<sup>†,‡</sup> and Yunqing Wang<sup>†</sup>

<sup>†</sup>Key Laboratory of Coastal Zone Environmental Processes, Yantai Institute of Coastal Zone Research, Chinese Academy of Sciences, Yantai 264003, China

<sup>‡</sup>Graduate University of Chinese Academy of Sciences, Beijing 100049, China

**ABSTRACT:** A highly sensitive surface-enhanced Raman scattering (SERS) platform for the selective trace analysis of As<sup>3+</sup> ions was reported based on glutathione (GSH)/4-mercaptopyridine (4-MPY)-modified silver nanoparticles (AgNPs). Here, GSH conjugated on the surface of AgNPs for specific binding with As<sup>3+</sup> ions in aqueous solution through As–O linkage and 4-MPY was used as a Raman reporter. When As<sup>3+</sup> ions were added to the system, the binding of As<sup>3+</sup> with GSH resulted in the aggregation of AgNPs, and excellent Raman signal of 4-MPY reporters was obtained which can reflect the concentration of As<sup>3+</sup> indirectly. Under optimal assay conditions, the limit of detection (LOD) was estimated to be as low as 0.76 ppb, which is lower than the WHO defined limit (10 ppb), and an excellent linear range of 4–300 ppb was obtained. The practical application had been carried out for determination of As<sup>3+</sup> in real water samples.

**KEYWORDS:** arsenic ion, surface-enhanced Raman scattering, silver nanoparticles, glutathione, 4-mercaptopyridine



## INTRODUCTION

Arsenic is a toxic substance with acute as well as chronic effects, and long-term exposure to arsenic can cause various cancers and other serious diseases.<sup>1</sup> The concentration of arsenic in the environment may be elevated because of certain anthropogenic activities and natural processes.<sup>1,2</sup> Arsenic contamination of drinking water has been prevalent around the world,<sup>3</sup> and as many as 140 million people worldwide may have been exposed to drinking water with arsenic contamination levels higher than the World Health Organization's (WHO) guideline of 10 ppb.<sup>4</sup> It is well-known that the major arsenic species found in environment samples are inorganic arsenite (As<sup>3+</sup>) and arsenate (As<sup>5+</sup>) salts, organic forms of arsenic, for example, dithioarsenate (DTA), dimethylarsenic acid (DMA) and monomethylarsenic acid (MMA).<sup>5,6</sup> Inorganic arsenic is more toxic than organic arsenic, and arsenite more toxic than arsenate.<sup>7</sup> Over the years, various analytical techniques for the detection of arsenic at the trace level have been developed, including atomic fluorescence spectrometry (AFS),<sup>8–10</sup> atomic absorption spectrometry (AAS),<sup>11,12</sup> inductively coupled plasma spectrometry (ICP) with optical emission detection<sup>13–15</sup> and high-performance liquid chromatography (HPLC) with optical spectrometry detection.<sup>16,17</sup> Although these methods can accurately measure arsenic in an environmental sample to microgram arsenic per liter concentrations, there is still a necessity for development of simple and rapid methods for field assays.<sup>18</sup>

Surface-enhanced Raman scattering (SERS) technique, which can be used in conjunction with commercially available portable Raman systems, has emerged as a potentially promising solution

due to its incomparable advantages. Since its discovery in the late 1970s,<sup>19–21</sup> SERS has been applied to a wide variety of biomedical and environmental analytical applications at the level of molecules, pathogens, cells and even whole living animals.<sup>22–25</sup> The two well-known mechanisms to account for the origin of SERS are the electromagnetic (EM) and chemical or charge transfer (CT) mechanisms.<sup>26,27</sup> SERS are extremely sensitive analytical techniques mainly based on the giant electromagnetic (EM) enhancement induced by nanostructured noble metal surfaces and associated to their localized plasmon resonance (LPR).<sup>26,28</sup> Apart from its high sensitivity, SERS possesses other intrinsic benefits, such as operation over a wide range of excitation wavelengths, reduced photobleaching and highly resolved spectroscopic bands. In recent years, several groups proposed SERS analysis methods based on metal nanoparticles. For example, Tsukruk and co-workers have introduced nanocanal arrays decorated with metal nanoparticles as efficient SERS substrates for trace-level detection of DNT;<sup>29</sup> Zamarion reported the SERS detection of hazardous metal ions (Hg<sup>2+</sup> and Cd<sup>2+</sup>) based on trimercaptotriazine-modified gold nanoparticles;<sup>30</sup> Dasary detected TNT using gold nanoparticles modified with cysteine for label-free SERS probe.<sup>31</sup> In the previous work, SERS have been used for detection of Hg<sup>2+</sup> ions in nanoliter droplets and melamine in milk powder solution based on gold nanoparticles.<sup>32,33</sup> Moreover, several other recent studies report trace analysis of glucose, gene diagnostics, and

**Received:** June 23, 2011

**Accepted:** September 14, 2011

**Published:** September 14, 2011

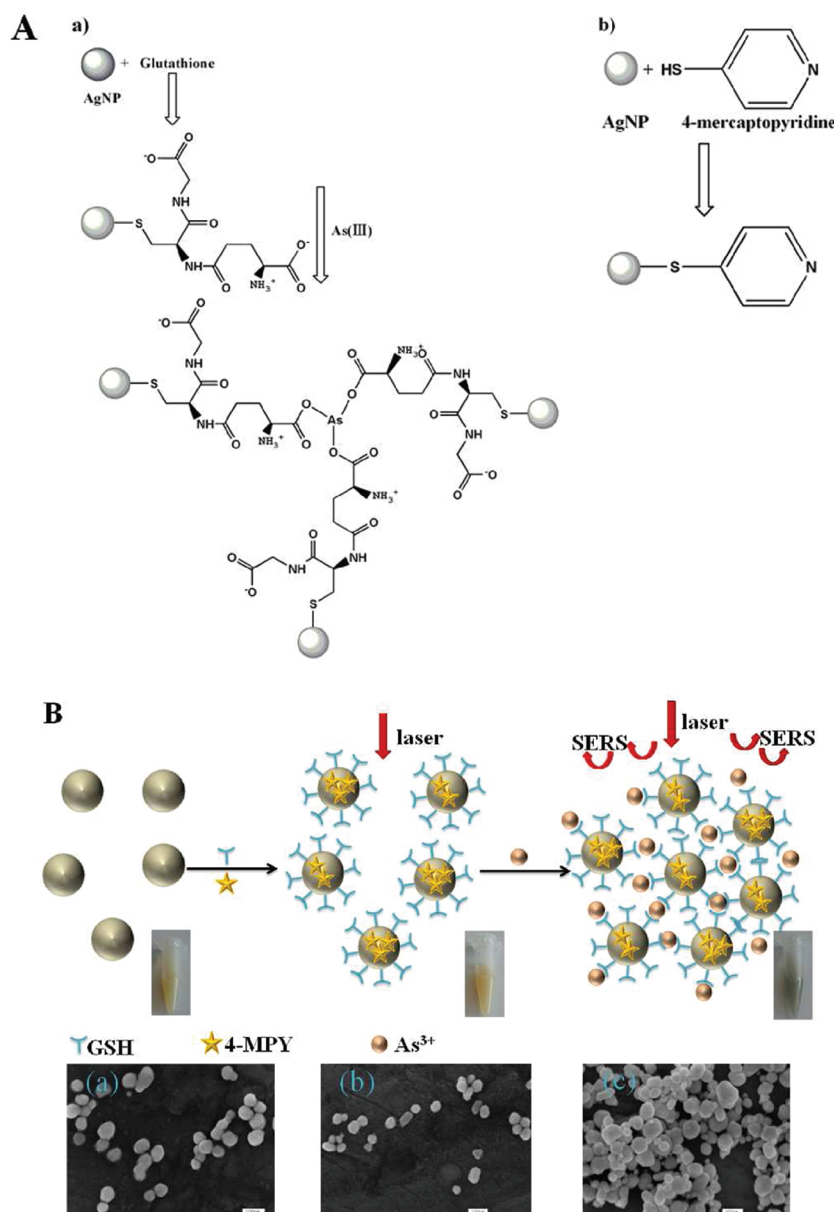


**Figure 1.** (A) Representation of AgNPs-based  $\text{As}^{3+}$  detection. a) GSH-modified AgNPs. b) 4-MPY-modified AgNPs. (B) Schematic diagram of the indirect SERS method for measuring  $\text{As}^{3+}$  using GSH/4-MPY-modified AgNPs. When  $\text{As}^{3+}$  ions were added to the system, the binding of  $\text{As}^{3+}$  with GSH caused the aggregation of AgNPs. The following is visual color changes and SEM images (scale bar, 100 nm) corresponding to (a) nonaggregated unmodified AgNPs, (b) nonaggregated GSH/4-MPY-modified AgNPs, and (c) aggregated GSH/4-MPY-modified AgNPs after addition of 200 ppb  $\text{As}^{3+}$ .

viruses.<sup>34</sup> In this paper, we demonstrated a highly sensitive SERS platform for the selective sensing of  $\text{As}^{3+}$  ions in aqueous media which is based on the use of GSH/4-MPY-modified silver nanoparticles (AgNPs). When the most moderate amount of GSH and 4-MPY were added to the silver colloid, the AgNPs were still monodispersed. Upon formation of As–O linkage, the distances among the AgNPs were shortened.<sup>35</sup> As a result, aggregation of AgNPs occurred, and the SERS signal increased significantly after the addition of  $\text{As}^{3+}$  ions. Crucially, the assay was both rapid and simple to implement and yielded the limit of detection (LOD) approximately 0.76 ppb. To the best of our knowledge, this is the first report on the SERS-based trace analysis of  $\text{As}^{3+}$  ions using GSH/4-MPY-modified AgNPs.

## EXPERIMENTAL SECTION

**Chemicals and Materials.** All chemicals used were of analytical grade or of the highest purity available. Silver nitrate ( $\text{AgNO}_3$ , 99.8%) and sodium hydroxide (NaOH, 96%) were obtained from Sinopharm Chemical Reagent Co. Ltd. (Shanghai, China), hydroxylamine hydrochloride ( $\text{NH}_2\text{OH}\cdot\text{HCl}$ ) was purchased from Tianjin Kermel Chemical Reagent Co. Ltd. (Tianjin, China) and used as received. Glutathione (GSH, 99%), 4-mercaptopyridine (4-MPY, 95%) were obtained from Sigma-Aldrich (USA). The concentration of  $\text{As}^{3+}$  stock solution purchased from SCP SCIENCE Co. Ltd. (Beijing, China) was 1000 ppm. The other metal salts were purchased from Beijing Chemical Reagent Company (Beijing, China). All glassware was thoroughly cleaned with Mill-Q ( $18\text{M}\Omega\text{ cm}^{-1}$  resistance) water

prior to use. Mill-Q water was used to prepare all the solutions in this study.

**Methods.** The morphology and size of the AgNPs, GSH/4-MPY-modified AgNPs were characterized by scanning electron microscopy (SEM) using a Hitachi-4800 scanning electron microscope operated at an accelerating voltage of 5 kV. SERS spectra were recorded using a Thermo Scientific Raman system RFS 100 equipped with a microscope and a 632.8 nm diode pumped He:Ne laser source and a power of 5mW.

**Preparation of AgNPs.** AgNPs were prepared by reducing silver nitrate using hydroxylamine hydrochloride at room temperature.<sup>36</sup> The advantages of the hydroxylamine hydrochloride-reduction are in its speed at room temperature and the fact that produced particles can be used for SERS measurements without further processing. First, 1 mL of  $3 \times 10^{-1}$  M NaOH was added to 9 mL of  $1.67 \times 10^{-2}$  M  $\text{NH}_2\text{OH} \cdot \text{HCl}$  to maintain an alkaline pH. Next, the solution was added rapid to 90 mL of  $1.11 \times 10^{-3}$  M  $\text{AgNO}_3$  solution with continuous stirring. The solution was continuously stirred for an additional one hour. The prepared silver colloid was stored at room temperature. UV/vis spectroscopy (not shown) and SEM were used to characterize the particle size of the produced colloids, and the average particle size was estimated to be  $65 \pm 5$  nm in diameter.

**Functionalization of AgNPs with GSH and 4-MPY.** The AgNP surfaces were modified by addition of GSH (100  $\mu\text{M}$ , 10  $\mu\text{L}$ ) and 4-MPY (500  $\mu\text{M}$ , 10  $\mu\text{L}$ ) to a solution of AgNPs (0.5 nM, 2 mL) with stirring for 2 h. The mixture was subsequently left for overnight without disturbance at room temperature.

**SERS Detection of  $\text{As}^{3+}$ .** The  $\text{As}^{3+}$  stock solution was used for the  $\text{As}^{3+}$  sensitivity studies. Various concentrations of  $\text{As}^{3+}$  were prepared using serial dilution of the stock solution to test the sensitivity limits of the GSH/4-MPY-modified AgNPs. Using the stock solution, we prepared 0.1–7 ppm of  $\text{As}^{3+}$  solutions. The SERS detection of aqueous  $\text{As}^{3+}$  was performed at ambient temperature. Briefly, 10  $\mu\text{L}$  of  $\text{As}^{3+}$  standard solution with different concentrations was added to 90  $\mu\text{L}$  of GSH/4-MPY-modified AgNP colloid. After incubating for 2 min, about 5  $\mu\text{L}$  of the above solution in the capillary tube was detected by laser Raman spectrometer.

## RESULTS AND DISCUSSION

**Mechanism for the Sensing System.** As displayed in Figure 1A(a), GSH can bind to AgNPs through Ag–S bonds.<sup>37,38</sup> It is reported that  $\text{As}^{3+}$  has a very high affinity for GSH ligand (The stability constant for  $\text{As}^{3+}$  ions and GSH is  $\log K = 32.0$ .<sup>39,40</sup>) and each  $\text{As}^{3+}$  ion can bind with three GSH-modified AgNPs through As–O linkage.<sup>41</sup> Figure 1B illustrated the schematic diagram of mechanism for  $\text{As}^{3+}$  detection using GSH/4-MPY-modified AgNPs. Unmodified AgNPs were well dispersed after synthesis because they were stabilized by negatively charged hydroxylamine chloride ions coating on their surface. During the process of SERS probe synthesis, Raman reporters 4-MPY could contact with AgNPs with Ag–S or Ag–N bond as Figure 1A(b).<sup>38</sup> By adjusting the adding amount of GSH and 4-MPY, the color of colloid was still yellow, which indicated that the GSH/4-MPY-modified AgNPs were well stabilized in the absence of  $\text{As}^{3+}$ . After addition of  $\text{As}^{3+}$ , the formation of As–O linkage led to dramatic aggregation of AgNPs which could be seen from the visible color change from yellow to brown. Meanwhile, the aggregated AgNPs could produce lots of hot spots, therefore the Raman scattering signal of 4-MPY increased significantly. The SEM images of the mono-dispersed AgNPs in  $\text{As}^{3+}$ -free solution and the aggregated AgNPs obtained after addition of  $\text{As}^{3+}$  were shown in Figure 1B(a–c).

The key idea to the current sensing method is the fact that aggregation of nanoparticles induces excellent enhancement of Raman signal from the 4-MPY reporters. This great enhancement is caused by the large electromagnetic field produced by hot spots,

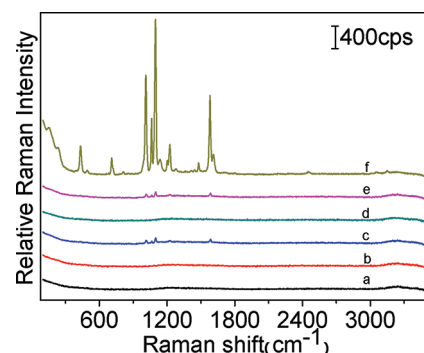


**Figure 2.** SERS spectra corresponding to (a) nonaggregated unmodified AgNPs without  $\text{As}^{3+}$ , (b) nonaggregated GSH-modified AgNPs without  $\text{As}^{3+}$ , (c) nonaggregated 4-MPY-modified AgNPs without  $\text{As}^{3+}$ , (d) aggregated GSH-modified AgNPs after addition of 100 ppb  $\text{As}^{3+}$ , (e) nonaggregated GSH/4-MPY-modified AgNPs without  $\text{As}^{3+}$  and (f) aggregated GSH/4-MPY-modified AgNPs after addition of 100 ppb  $\text{As}^{3+}$ .

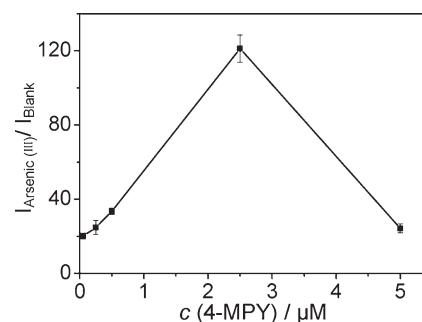


**Figure 3.** Effect of the concentration of 4-MPY (from 0.05  $\mu\text{M}$  to 5  $\mu\text{M}$ ) of the sensing system on the Raman signal intensity in the presence of 500 nM GSH and 500 ppb  $\text{As}^{3+}$ . The incubation time was 2 min.

which resides in the nanoscale junctions in metal nanostructures. According to recent SERS data reported by Kneipp et al., the SERS enhancement factor for silver nanoclusters was found to be 7 orders of magnitude higher than the enhancement factor for isolated AgNPs.<sup>42</sup> Accordingly, the recovered SERS signal of Raman reporters (4-MPY) was significantly increased as the aggregation of AgNPs after the addition of  $\text{As}^{3+}$  ions.

**Effect of the Concentration of 4-MPY and GSH.** Raman reporter played an important role in SERS-based assay. In order to acquire satisfactory detection sensitivity for  $\text{As}^{3+}$  ions, 4-MPY as the Raman reporter was chosen in this study. Meanwhile unmodified AgNPs and GSH-modified AgNPs were also tested for control experiments. Although GSH-modified AgNPs could aggregate after addition of  $\text{As}^{3+}$  ions, there was no apparent SERS signal (Figure 2), which illustrated that the indirect SERS sensing method using 4-MPY as Raman reporter was much sensitive than the direct sensing way.

The effect of the concentration of the reporter on SERS signal intensity was investigated. Five different concentrations of 4-MPY ranging from 0.05  $\mu\text{M}$  to 0.5  $\mu\text{M}$  were tested, and the corresponding Raman spectra were shown in Figure 3. It was found that the largest signal was achieved with 2.5  $\mu\text{M}$  4-MPY. When the concentration of 4-MPY was increased further, there was no obvious enhancement of the signal. Moreover, a higher concentration of 4-MPY would also induce AgNPs aggregation. Thus, a concentration of 2.5  $\mu\text{M}$  was selected for 4-MPY throughout the study.

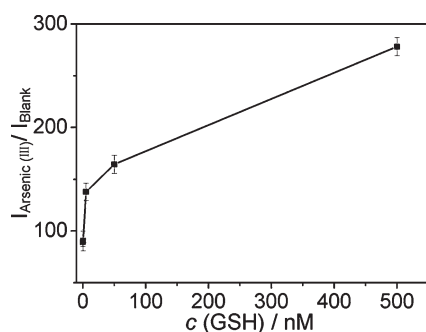


**Figure 4.** Effect of the concentration of GSH (from 0.05 to 500 nM) of the sensing system on the Raman signal intensity in the presence of 2.5  $\mu\text{M}$  4-MPY and 300 ppb  $\text{As}^{3+}$ . The incubation time was 2 min.

We further studied the effect of the GSH concentration (from 0.05 nM to 500 nM) on SERS signal intensity, and the corresponding Raman spectra were performed in Figure 4. It could be seen that the SERS signal became larger and larger with the concentration of GSH increasing. Moreover, when higher concentration of GSH (>500 nM) was added to the AgNPs solution, the colloid solution became brown immediately. It indicated that higher concentration of GSH would induce AgNPs aggregation because more GSH would replace the negatively charged hydroxylamine chloride ions coating on their surface and affect the stability of AgNPs. Thus, a concentration of 500 nM of GSH was used throughout the rest of the study.

**Sensitivity of the Sensor.** SERS spectra of GSH/4-MPY-modified AgNPs with different  $\text{As}^{3+}$  ion concentrations were shown in Figure 5A and Figure 5B. There are many spectra features that are characteristic of 4-MPY which can be used for indirect quantitative determination of  $\text{As}^{3+}$  ions, such as those at 712, 1018, 1067, 1100, 1280, 1589, and 1614  $\text{cm}^{-1}$ . The strongly enhanced band at 1100  $\text{cm}^{-1}$  corresponding to the ring-breath/C–S stretching mode indicates that 4-MPY is adsorbed onto the surfaces of the AgNPs through the sulfur atom.<sup>43,44</sup> This is also supported by the C–S stretching mode at 712  $\text{cm}^{-1}$ , which displays an increase in intensity. The band at 1589 and 1614  $\text{cm}^{-1}$  correspond to the C–C stretching mode, and C–H mode bands at 1067 and 1280  $\text{cm}^{-1}$  are also observed. The band at 1018  $\text{cm}^{-1}$  is related to ring-breathing vibrations. It can be seen that average SERS intensities for all peaks increase as a function of  $\text{As}^{3+}$  ion concentration. According to the spectra, the peak around 1018  $\text{cm}^{-1}$  was the most prominent one, and its intensity was very sensitive to the concentration of  $\text{As}^{3+}$  ions. Therefore, it was selected as an instructive peak for the quantitative analysis of  $\text{As}^{3+}$  ions. This relationship is expounded in Figure 5C where the variation in the intensity of the 1018  $\text{cm}^{-1}$  4-MPY peak is plotted as a function of  $\text{As}^{3+}$  ion concentration. It can be seen that good linearity is observed for  $\text{As}^{3+}$  ion concentration up to 300 ppb ( $R = 0.9977$ ) (inset of Figure 5C). Additionally, the LOD (based on a minimum signal-to-noise ratio of 3) was calculated to be 0.76 ppb. This confirms the exquisite sensitivity of the assay, and more importantly yields a limit of detection below the WHO defined limit of 10 ppb in drinking water.

**Selectivity of the Sensor.** Under optimized conditions, we investigated the selectivity of our approach toward 100 ppb  $\text{As}^{3+}$  ions (1.34  $\mu\text{M}$ ) against other metal ions ( $\text{Cd}^{2+}$ ,  $\text{Cu}^{2+}$ ,  $\text{Cr}^{3+}$ ,  $\text{Zn}^{2+}$ ,  $\text{Ni}^{2+}$ ,  $\text{Fe}^{3+}$ ,  $\text{As}^{5+}$  at a concentration of 1.34  $\mu\text{M}$ , and  $\text{K}^+$ ,  $\text{Hg}^{2+}$ ,  $\text{Mg}^{2+}$ ,  $\text{Pb}^{2+}$ ,  $\text{Ca}^{2+}$ ,  $\text{Mn}^{2+}$  at a concentration of 13.4  $\mu\text{M}$ ). As shown in Figure 6, only the addition of  $\text{As}^{3+}$  ions could induce the aggregation

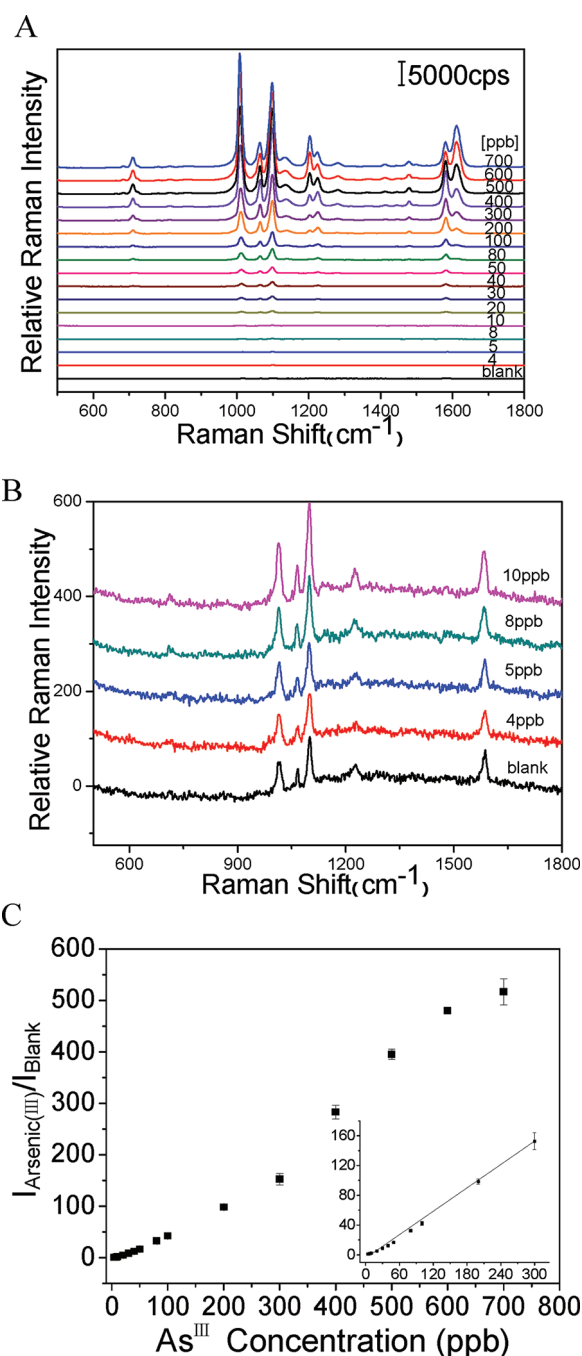


**Figure 5.** (A) SERS spectra changes of GSH/4-MPY-modified AgNPs with different  $\text{As}^{3+}$  ion concentrations, (B) SERS spectra changes of GSH/4-MPY-modified AgNPs at lower concentrations of  $\text{As}^{3+}$  ion and (C) plots of corresponding intensity of the Raman band centered at 1011  $\text{cm}^{-1}$  as a function of  $\text{As}^{3+}$  concentration. Inset shows a linear relationship in the lower concentration range from 4 to 300 ppb ( $R = 0.9977$ ). The error bars represent standard deviations based on three independent measurements. The incubation time was 2 min.

of AgNPs through the coordination of GSH and  $\text{As}^{3+}$  ions, resulting in a significant increase of the SERS signals. This indicated that our system could respond toward  $\text{As}^{3+}$  ions with high selectivity.

**Practical Application.** To test the practicality of the developed sensing platform, we prepared a series of samples by spiking

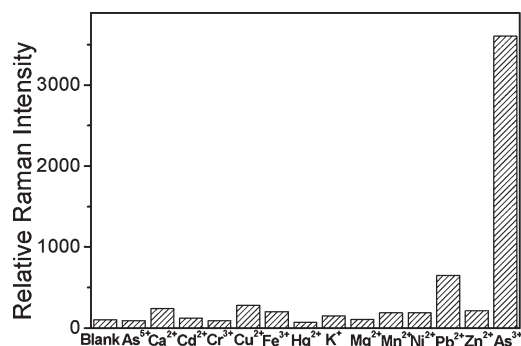


**Figure 6.** Metal ion-induced SERS intensity changes of proposed  $\text{As}^{3+}$  SERS sensor. Inset shows the SERS spectra changes upon kinds of metal ions. The concentration of  $\text{As}^{3+}$ ,  $\text{Cd}^{2+}$ ,  $\text{Cu}^{2+}$ ,  $\text{Cr}^{3+}$ ,  $\text{Zn}^{2+}$ ,  $\text{Ni}^{2+}$ ,  $\text{Fe}^{3+}$ , and  $\text{As}^{5+}$  were  $1.34 \mu\text{M}$ , that is  $100 \text{ ppb}$   $\text{As}^{3+}$ . And other metal ions concentrations were  $13.4 \mu\text{M}$ . The incubation time was 2 min.

**Table 1.** Determination of  $\text{As}^{3+}$  in Drinking Water by Standard Addition Method

sample mean $\pm$ SD	added (ppb)	found (ppb)	recovery (%)
1	15.0	$14.8 \pm 0.50$	98.4
2	25.0	$24.5 \pm 0.86$	98.1
3	90.0	$93.7 \pm 2.30$	104.1

standard  $\text{As}^{3+}$  solution to drinking water to mimic the  $\text{As}^{3+}$  ions contaminated water. The drinking water, KunYu mountain drinking mineral water, was directly analyzed without treatment, which is reported to contain  $\text{Sr}^{2+}$  (0.2–0.6 mg/L),  $\text{K}^+$  (0.1–0.8 mg/L),  $\text{Na}^+$  (32.2–42.9 mg/L),  $\text{Mg}^{2+}$  (3.5–7.0 mg/L),  $\text{SO}_4^{2-}$  (5.0–17.8 mg/L),  $\text{Cl}^-$  (31.5–43.3 mg/L), and so on. So, it suggested that trace detection of  $\text{As}^{3+}$  from mixed ion water solutions were performed. Excellent recoveries were obtained, including 98.4, 98.1, and 104.1% for the spiked drinking mineral water samples with 15, 25, and 90 ppb  $\text{As}^{3+}$  standard solution, respectively (Table 1). It indicated this method could serve as a practical and convenient method for the primary screening of  $\text{As}^{3+}$  ions pollution.

## CONCLUSIONS

In the present work, we have successfully demonstrated a highly sensitive and selective method for the detection of  $\text{As}^{3+}$  ions in aqueous media via SERS technique. The experimental results showed that  $\text{As}^{3+}$  could be detected quickly and accurately against other metal ions. A high sensitivity (LOD 0.76 ppb) and wide linear range (4–300 ppb) was obtained. We validated its practicality through analysis of drinking water sample and obtained satisfying results. This simple, rapid, cost-effective, sensitive, and selective sensing system holds great potential for practical application.

## AUTHOR INFORMATION

### Corresponding Author

\*E-mail: lxchen@yic.ac.cn.

## ACKNOWLEDGMENT

This study was financially supported by the National Natural Science Foundation of China (20975089), the Innovation Projects of the Chinese Academy of Sciences (KZCX2-EW-206), the

Department of Science and Technology of Shandong Province of China (2008GG20005005), and the 100 Talents Program of the Chinese Academy of Sciences.

## REFERENCES

- (1) Mohan, D.; Pittman, C. U., Jr. *J. Hazard. Mater.* **2007**, *142*, 1–53.
- (2) Smedley, P. L.; Kinniburgh, D. G. *Appl. Geochem.* **2002**, *17*, 517–568.
- (3) National Research Council; *Arsenic in Drinking Water*; National Academy Press: Washington, D. C., 1999.
- (4) <http://www.who.int/mediacentre/factsheets/fs210/en>.
- (5) Moriarty, M. M.; Koch, I.; Gordon, R. A.; Reimer, K. J. *Environ. Sci. Technol.* **2009**, *43*, 4818–4823.
- (6) Cullen, W. R.; Reimer, K. J. *Chem. Rev.* **1989**, *89*, 713–764.
- (7) Yokel, R. A.; Lasley, S. M.; Dorman, D. C. *J. Toxicol. Environ. Health, Part B: Crit. Rev.* **2006**, *9*, 63–85.
- (8) Zhang, N.; Fu, N.; Fang, Z.; Feng, Y.; Ke, L. *Food Chem.* **2011**, *124*, 1185–1188.
- (9) Liu, L.; Zhou, Q.; Zheng, C.; Hou, X.; Wu, L. *Atom. Spectrosc.* **2009**, *30*, 59–64.
- (10) Ito, K.; Palmer, C. D.; Corns, W. T.; Parsons, P. J. *J. Anal. Atom. Spectrom.* **2010**, *25*, 822–830.
- (11) Sounderajan, S.; Udas, A. C.; Venkataramani, B. *J. Hazard. Mater.* **2007**, *149*, 238–242.
- (12) Pantuzzo, F. L.; Silva, J. C. J.; Ciminelli, V. S. T. *J. Hazard. Mater.* **2009**, *168*, 1636–1638.
- (13) Jitmanee, K.; Oshima, M.; Motomizu, S. *Talanta* **2005**, *66*, 529–533.
- (14) Gil, R. A.; Ferrua, N.; Salonia, J. A.; Martinez, L. D. *J. Hazard. Mater.* **2007**, *143*, 431–436.
- (15) Dufailly, V.; Noel, L.; Guerin, T. *Anal. Chim. Acta* **2008**, *611*, 134–142.
- (16) Al-Assaf, K. H.; Tyson, J. F.; Uden, P. C. *J. Anal. Atom. Spectrom.* **2009**, *24*, 376–384.
- (17) Carmen, M. P.; Jorge, M. P.; Purificacion, L. M.; Soledad, M. L.; Esther, F. F.; Dario, P. R. *J. Chromatogr. A* **2008**, *1215*, 15–20.
- (18) Melamed, D. *Anal. Chim. Acta* **2005**, *532*, 1–13.
- (19) Fleischmann, M.; Hendra, P. J.; McQuillan, A. *J. Chem. Phys. Lett.* **1974**, *26*, 163–166.
- (20) Jeanmaire, D.; Van Duyne, R. J. *Electroanal. Chem.* **1977**, *84*, 1–20.
- (21) Chen, L.; Choo, J. *Electrophoresis* **2008**, *29*, 1815–1828.
- (22) Park, H.; Lee, S.; Chen, L.; Lee, E. K.; Shin, S. Y.; Lee, Y. H.; Son, S. W.; Oh, C. H.; Song, J. M.; Kang, S. H.; Choo, J. *Phys. Chem. Chem. Phys.* **2009**, *11*, 7444–7449.
- (23) Qian, X.; Peng, X. H.; Ansari, D. O.; Yin-Geon, Q.; Chen, G. Z.; Shin, D. M.; Yang, L.; Young, A. N.; Wang, M. D.; Nie, S. *Nat. Biotechnol.* **2008**, *26*, 83–90.
- (24) Lee, S.; Choi, J.; Chen, L.; Park, B.; Kyong, J. B.; Seong, G. H.; Choo, J.; Lee, Y.; Shin, K. H.; Lee, E. K.; Joo, S. W.; Lee, K. H. *Anal. Chim. Acta* **2007**, *590*, 139–144.
- (25) Jarvis, R. M.; Goodacre, R. *Chem. Soc. Rev.* **2008**, *37*, 931–936.
- (26) Moskovits, M. *Rev. Mod. Phys.* **1985**, *57*, 783–826.
- (27) Otto, A.; Mrozek, I.; Grabhorn, H.; Akemann, W. *J. Phys. Condens. Mater.* **1992**, *4*, 1143–1212.
- (28) Aroca, R. *Surface-Enhanced Vibrational Spectroscopy*; John Wiley & Sons: Chichester, U.K., 2006.
- (29) Ko, H.; Tsukruk, V. V. *Small* **2008**, *4*, 1980–1984.
- (30) Zamarlon, V. M.; Tlmm, R. A.; Arakl, K.; Toma, H. E. *Inorg. Chem.* **2008**, *47*, 2934–2936.
- (31) Dasary, S. S. R.; Singh, A. K.; Senapati, S.; Yu, H. T.; Ray, P. C. *J. Am. Chem. Soc.* **2009**, *131*, 13806–13812.
- (32) Wang, G.; Lim, C.; Chen, L.; Chon, H.; Choo, J.; Hong, J.; de Mello, A. J. *Anal. Bioanal. Chem.* **2009**, *394*, 1827–1832.
- (33) Lou, T. T.; Wang, Y. Q.; Li, J. H.; Peng, H. L.; Xiong, H.; Chen, L. X. *Anal. Bioanal. Chem.* **2011**, *401*, 333–338.

- (34) Ko, H.; Singamaneni, S.; Tsukruk, V. V. *Small* **2008**, *4*, 1576–1599.
- (35) Kalluri, J. R.; Arbnesi, T.; Khan, S. A.; Neely, A.; Candice, P.; Varisli, B.; Washigton, M.; McAfee, S.; Robinson, B.; Banerjee, S.; Singh, A. K.; Senapati, D.; Ray, P. C. *Angew. Chem., Int. Ed.* **2009**, *48*, 9668–9671.
- (36) Leopold, N.; Lendl, B. *J. Phys. Chem. B* **2003**, *107*, 5723–5727.
- (37) Chen, Z.; He, Y. J.; Luo, S. L.; Lin, H. L.; Chen, Y. F.; Sheng, P. T.; Li, J. X.; Chen, B. B.; Liu, C. B.; Cai, Q. Y. *Analyst* **2010**, *135*, 1066–1069.
- (38) Mo, L. X.; Liu, D. Z.; Li, W.; Li, L. H.; Wang, L. C.; Zhou, X. Q. *Appl. Surf. Sci.* **2011**, *257*, 5745–5753.
- (39) Rey, N. A.; Howarth, O. W.; Pereira-Maia, E. C. *J. Inorg. Biochem.* **2004**, *98*, 1151–1159.
- (40) Burford, N.; Eelman, M. D.; Groom, K. J. *Inorg. Biochem.* **2005**, *99*, 1992–1997.
- (41) Kalluri, J. R.; Arbnesi, T.; Khan, S. A.; Neely, A.; Candice, P.; Varisli, B.; Washington, M.; McAfee, S.; Robinson, B.; Banerjee, S.; Singh, A. K.; Senapati, D.; Ray, P. C. *Angew. Chem., Int. Ed.* **2009**, *48*, 9668–9671.
- (42) Kneipp, K.; Kneipp, H.; Kneipp, J. *Acc. Chem. Res.* **2006**, *39*, 443–450.
- (43) Wang, W. Q.; Li, W. L.; Zhang, R. F. *Mater. Chem. Phys.* **2010**, *124*, 385–388.
- (44) Guo, H.; Ding, L.; Mo, Y. J. *J. Mol. Struct.* **2011**, *991*, 103–107.